NANO LETTERS

Letter

pubs.acs.org/NanoLett

Charge Transport Characteristics of Diarylethene Photoswitching Single-Molecule Junctions

Youngsang Kim,[†] Thomas J. Hellmuth,[‡] Dmytro Sysoiev,[§] Fabian Pauly,[‡,⊥] Torsten Pietsch,[†] Jannic Wolf,[§] Artur Erbe,[∥] Thomas Huhn,[§] Ulrich Groth,[§] Ulrich E. Steiner,[§] and Elke Scheer*[,†]

[†]Department of Physics, University of Konstanz, 78457 Konstanz, Germany

[‡]Institut für Theoretische Festkörperphysik and DFG Center for Functional Nanostructures, Karlsruhe Institute of Technology, 76128 Karlsruhe, Germany

[§]Department of Chemistry, University of Konstanz, 78457 Konstanz, Germany

[∥]Helmholtz-Zentrum Dresden Rossendorf, 01328 Dresden, Germany

S *Supporting Information*

ABSTRACT: We report on the experimental analysis of the charge transport through single-molecule junctions of the open and closed isomers of photoswitching molecules. Sulfur-free diarylethene molecules are developed and studied via electrical and optical measurements as well as density functional theory calculations. The single-molecule conductance and the current−voltage characteristics are measured in a mechanically controlled break-junction system at low temperatures. Comparing the results with the single-level transport model, we find an unexpected behavior of the current-dominating molecular orbital upon isomerization. We show that both the side chains and end groups of the molecules are crucial to understand the charge transport mechanism of photoswitching molecular junctions.

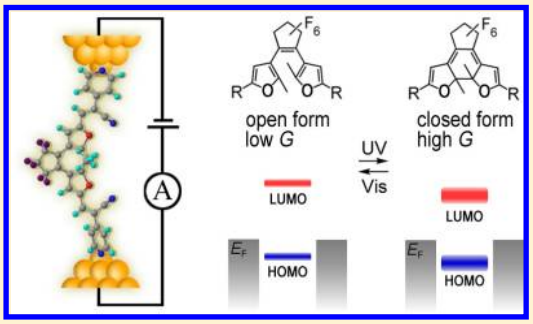

KEYWORDS: *Photochromic, diarylethene, single molecule, charge transport, single-level model, low temperature*

Charge transport in organic molecules is actively explored toward the realization of novel electronic circuits and computational devices.[1−5] Recently, the field of molecular electronics has been investigated extensively to understand novel physical phenomena, which arise when external stimuli such as electrochemical gating,[6−8] electric field gating,[4,9] mechanical stretching,[10−12] magnetic fields,[13−16] and light irradiation[3,14,17,18] are present. In particular, optically switchable diarylethene molecules, among other photochromic molecules[19] (e.g., azobenzenes, stilbenes, and spiropyrans), are promising building blocks for electronic circuit elements due to their excellent thermal stability, high fatigue resistance, and negligible change of length between both states.[20,21] Since the electrical characterization of diarylethene molecules has started, measurements of the charge transport properties of molecular ensembles using large-area samples,[22] molecular networks with nanoparticles,[17] atomic force microscope techniques,[23] carbon nanotube junctions,[19] and structural studies using the scanning tunneling microscope[24,25] have been performed successfully. In addition, mechanically controlled break-junctions (MCBJs)[11,18] and modified scanning-tunneling-microscope break-junctions[26] were applied to create diarylethene single-molecule contacts at room temperature.

However, up to now low-temperature charge transport experiments using photochromic single-molecule junctions have not been performed, although the understanding of the charge transport behavior under these controlled conditions is of importance to design molecules that show improved switching properties when contacted by metallic electrodes. The sulfur atoms in the switching core (i.e., in thiophene rings) may bind to metallic surfaces (i.e., Au),[27−29] causing contact configurations unsuitable for photoexcitation.[18,30] In addition, a strong, direct electronic coupling between the electrodes and the switching core may quench the photoexcitation, effectively hindering the switching process.[31]

Reversible switching of sulfur-containing analogues was so far observed in molecular ensembles and arrays only.[17,22] There were a few attempts to switch the conductance of single-molecule junctions in both directions.[18] However, continuous reversible switching of photochromic single-molecule junctions between two measurable conductance levels remains a challenge. The most severe problems in this context include the enhancement of the quantum yield of the photoreaction and the improvement of the alignment of the Fermi energy (E_F) compared to the HOMO and lowest unoccupied molecular orbital (LUMO) levels while preserving the molecular switching behavior, i.e., avoiding a relaxation of excited electrons back to the initial ground state resulting in no change of the molecular geometry upon light irradiation.[18] We

Received: April 25, 2012

   dx.doi.org/10.1021/nl3015523 | *Nano Lett.* XXXX, XXX, XXX−XXX

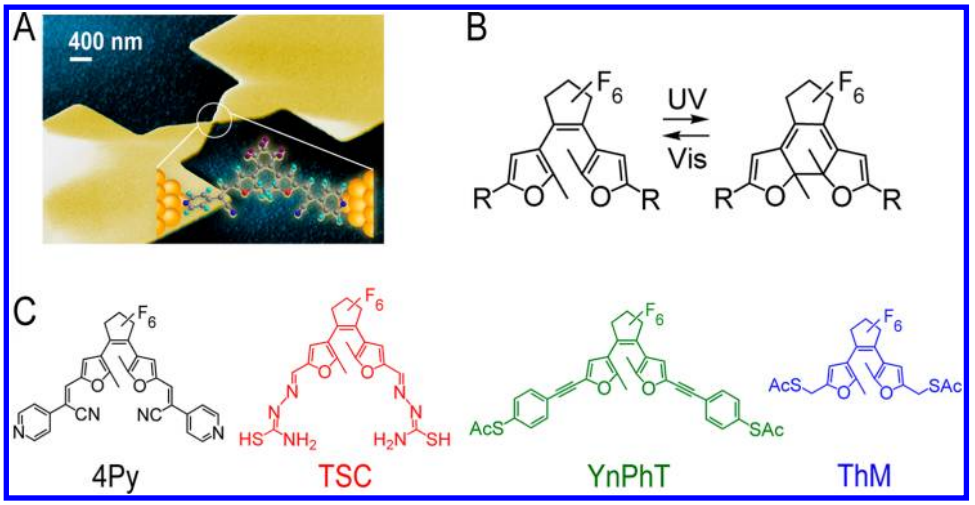

Figure 1. (A) Scanning electron micrograph of the MCBJ device and an illustration of a Au−4Py−Au junction. (B) Sketches of open (left) and closed (right) forms of photochromic molecules (difurylethenes); R indicates the extended side chains and end groups. (C) Structures of the four different molecules, 4Py (black), TSC (red), YnPhT (green), and ThM (blue), measured in this study.

note that the demand to achieve a high switching ratio (SR) of conductance values, and hence a good electronic transport in the "on" state, is to some extent conflicting with the reduced electronic coupling required to preserve molecular function, i.e., not to quench the photoexcitation processes.

Therefore, the development of photochromic molecules the switching core of which is sulfur-free, in combination with proper side chains and end groups represents a crucial step toward a high switching yield and reversible switching.[30] Furthermore, for the case of transport being mediated by the highest occupied molecular orbital (HOMO), in general one expects that the HOMO level shifts toward the Fermi energy E_F, when the central ring of the switching core closes. Nevertheless, there are a few theoretical reports indicating an unconventional shift of the current-dominating molecular orbital (frontier MO) between open and closed isomers.[32]

To this end, we investigate charge transport through new sulfur-free diarylethene-derivative molecules in a MCBJ system at low temperatures. The chemical synthesis of several members of this new class of molecules has been carried out, and their properties have been analyzed using NMR, UV/vis measurements, and density functional theory. The single-molecule conductance and the current−voltage (I−V) characteristics of four different molecules are reported here. From these studies, we determine the position of the current-dominating molecular level (E_0) with respect to E_F and its broadening (Γ) within the framework of the single-level transport model.[2,11,33−35] While the various side chains and end groups were designed to overcome the quenching problem, our results reported below will show that further improvements are still needed in terms of their conductance values and the related SR.

The photochromic single-molecule device used in this study is sketched in Figure 1A. A single diarylethene molecule bridges the gold electrodes at low temperature in cryogenic vacuum conditions. The open and closed forms of diarylethene are shown in Figure 1B. The open isomer closes the central ring under UV light irradiation leading to a completely π-conjugated current path along the molecule, while the closed isomer opens the ring under visible light irradiation, breaking up the current path into two rather decoupled systems. The π-conjugation through the entire molecule in the closed form is supposed to lead to a higher conductance than for the broken π-system. We report here measurements carried out on the four species labeled 4Py, TSC, YnPhT, and ThM as shown in Figure 1C.[30] The details of the chemical properties of 4Py and TSC and the applied synthetic methods have been described in part in ref 30 and are presented together with those of YnPhT and ThM in the Supporting Information. UV/vis absorption spectroscopy was performed to characterize the optical properties of each type of molecule (see Supporting Information). The open forms isomerize to the closed form upon UV light (313 nm) irradiation. However, slight differences between the molecules are perceived for the reverse reaction. In general, molecules with a conjugated side chain such as 4Py, TSC, and YnPhT react to visible light around 570−630 nm wavelength, while the ThM molecule, containing a nonconjugated side-chain, is triggered at ∼460 nm. We attribute this difference to the spatial extent of the π-electron system, which is smallest for ThM. The longest-wavelength absorption edge is indicative of the possible optical excitation with lowest energy. A variation in the absorption band thus suggests a variation of the HOMO−LUMO gap of the molecules.[36] As expected, the open forms show higher excitation energies, indicating larger HOMO−LUMO gaps than the closed forms, and the ThM molecules containing nonconjugated side chains exhibit larger gaps in both open and closed form than the respective molecules with conjugated side chains. This is in agreement with our theoretical calculations of the isolated molecules using density functional theory (see Supporting Information). Hence, the optical measurements and electronic properties suggest that we may divide the difurylethenes molecules into those containing conjugated (4Py, TSC, and YnPhT) and nonconjugated (ThM) side chains.

The HOMO−LUMO gaps of isolated molecules do not correlate directly with the electrical measurement. However, on the basis of optical properties and the inferred trends in HOMO−LUMO gaps within the class of difurylethenes, we can carefully assume similar trends for the electrical measurements. To be explicit, we expect a different behavior for the molecules containing conjugated side chains (4Py, TSC, and YnPhT) and the molecules containing nonconjugated side chains (ThM).

Prior to mounting the nanofabricated samples in a custom-designed cryogenic vacuum insert equipped with a MCBJ

dx.doi.org/10.1021/nl3015523 | Nano Lett. XXXX, XXX, XXX−XXX

system, the molecules are switched to either the open or the closed form in ethanol and are assembled on the sample. The acetyl groups at the ends of YnPhT and ThM are deprotected with ammonium hydroxide (NH_4OH) forming a thiol (−SH) group before assembling on the gold surfaces.[37] All electrical measurements are performed at 4.2 K in a helium environment. Upon stretching of the metallic bridge, the last single-atom Au−Au contact breaks at a conductance G of $\sim 1G_0$ with $G_0 = 2e^2/h$, the quantum of conductance. Next, if a molecule is trapped in the junction, the conductance drops fast to a value corresponding to the molecular conductance. Upon further stretching, the conductance reveals a plateau, i.e., comparatively small changes of G with distance, before the metal−molecule−metal contact finally breaks and the conductance drops below $10^{-8}G_0$. This procedure is reversed by closing the junction until Au−Au contacts develop and a conductance of $\sim 1G_0$ is observed. Further closing increases the conductance in steps of the order of G_0 as expected for Au atomic size contacts. Typical conductance traces for the open and closed forms of the four different molecules are displayed in Figures 2A and 2B,

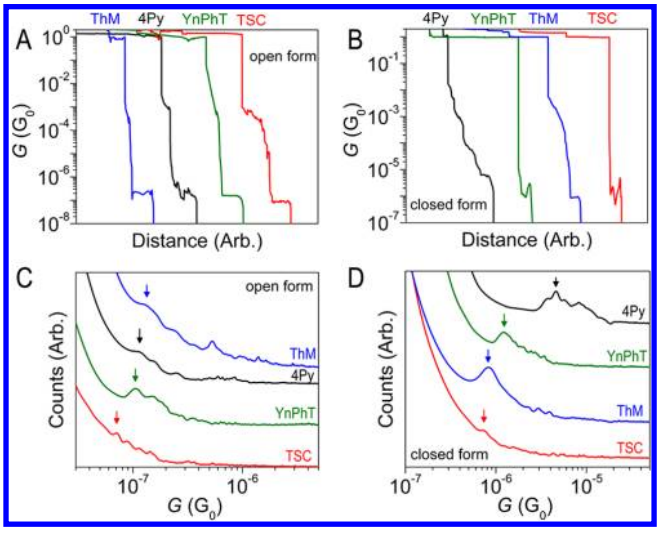

Figure 2. (A, B) Typical conductance−distance traces and (C, D) conductance histograms of photochromic molecular junctions for open and closed forms of all four molecules as indicated in the panels. The arrows point at the prominent conductance peak of the histograms in the lowest conductance regime for each molecular junction. The histograms are collected by repeating the breaking and closing process about 1000 times for the open and closed forms of each molecule.

respectively. For both states of each molecule, the junction is opened and closed repeatedly about 1000 times to determine the preferred single-molecule conductance. The respective histogram graphs with linear-binning are plotted in Figures 2C and 2D for the open and closed forms. The lowest preferred conductance values of each state, indicated by arrows in Figures 2C and 2D, are given in Table 1. These values are obtained by fitting a Lorentzian to the maximum of the histograms in the lowest conductance regime, and the error range of the conductance is defined by the half-width at half-maximum (HWHM). The appearance of multiple conductance peaks in the histograms can be attributed to the formation of contact geometries with different configurations of the molecule, of the electrodes, or at the molecule−electrode interface.[10,12] Furthermore, the maxima at higher conductance values may correspond to junctions containing multiple molecules contributing to the current.[38−40] We observe that the histograms of TSC feature only several faint maxima, presumably because of the complexity of the side chains enabling a larger amount of nearly isoenergetic contact configurations. Here we restrict ourselves to the investigation of junctions with the lowest stable conductance as indicated by the position of the lowest-conductance peak. They are supposed to correspond to straight single-molecule junctions. As expected, the single-molecule conductance of the closed form is higher in all cases than that of the open form. As indicated in Figure 1C, the 4Py molecule is equipped with side chains consisting of pyridine end groups. They establish a very direct link between the molecular π-system and the metallic surfaces.[41,42] This leads to a relatively large SR of the conductance, i.e., the high ratio between the single-molecule conductance in the closed form and that in the open form (see Table 1). In contrast, the other molecules show a configuration, where the side chains are electronically more separated from the end groups leading to an effective barrier and voltage drop between side chains and end groups and thus a significant reduction of the SR. Hence, the ThM molecule featuring a saturated CH_2 side chain shows the lowest SR. In general, we find that the SR of photochromic molecules is determined by the degree of the π-conjugation on both the end group and the side chain, which is consistent with the theoretical results of ref 43.

To understand the charge transport mechanism for the molecular junctions, we measured the $I-V$ characteristics of the open and closed isomers and then constructed density plots of $I-V$ curves as shown in Figure 3. In order to reveal the transport mechanism, we studied exemplarily the $I-V$s of 4Py and ThM molecules between 4.2 and 40 K and found them to be temperature independent, demonstrating that coherent tunneling is the dominant charge transport mechanism (see Supporting Information). In Figure 3, the intensity of the color is indicative of the probability to find the respective $I(V)$ values.

Table 1. Length of the Molecules in Their Open and Closed Forms, Conductance Values, and Conductance Switching Ratios[a]

	length of molecule (Å)		conductance (G_0)		
	open form	closed form	open form	closed form	conductance switching ratio
4Py	19.05	16.66	$(1.2 \pm 0.5) \times 10^{-7}$	$(4.6 \pm 0.9) \times 10^{-6}$	38.3 ± 17.6
TSC	16.45	16.04	$(7.2 \pm 3.2) \times 10^{-8}$	$(7.5 \pm 1.9) \times 10^{-7}$	10.4 ± 5.3
YnPhT	22.80	19.77	$(1.1 \pm 0.2) \times 10^{-7}$	$(1.3 \pm 0.4) \times 10^{-6}$	11.8 ± 4.2
ThM	9.46	8.64	$(1.4 \pm 1.0) \times 10^{-7}$	$(8.3 \pm 4.5) \times 10^{-7}$	5.9 ± 5.3

[a]Molecular lengths are obtained by calculating the structure of the isolated molecules. For 4Py we measure the longest distance between nitrogen atoms, and for the other molecules we show the distance between terminal sulfurs (see Supporting Information). Conductance values are obtained from Figure 2c,d by fitting a Lorentzian function to the lowest conductance maximum.

dx.doi.org/10.1021/nl3015523 | Nano Lett. XXXX, XXX, XXX−XXX

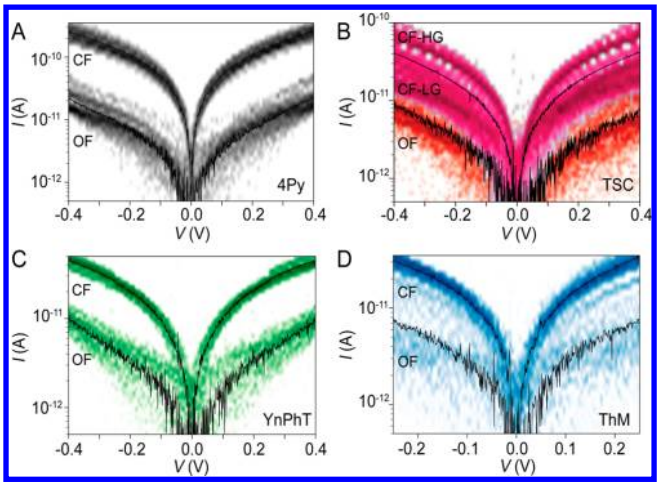

Figure 3. Density plots of about 20 $I-V$ curves of the open form (OF) and the closed form (CF) are displayed for (A) 4Py, (B) TSC, (C) YnPhT, and (D) ThM. The density plots are obtained by 100 by 100 bins for I and V, and the color indicates counts in log-scale (minimum (white) is below 3 counts and maximum (dark color) is 60 counts). The solid curves are the averaged $I-V$s for each isomer. In panel B, CF-HG and CF-LG indicate the high conductance and the low conductance states of closed TSC, respectively, which we attribute to the coupling of TSC to gold via different end groups.

The $I-V$s are obtained at the last conductance plateau (i.e., for the single-molecule contact). The high and low conductance $I-V$s are measured with closed and open isomers, respectively. The distributions of $I-V$s of open and closed isomers of TSC and ThM in Figures 3B and 3D are not clearly separated due to the low SR. Moreover the $I-V$ distribution for TSC in Figure 3B is relatively broad due to the wide distribution of single-molecule conductance values (see Table 1). It splits into two groups [i.e., high (HG) or low (LG) conductance] for the closed form which, however, cannot be distinguished in the conductance histogram of Figure 2D. We observe that in the LG state the $I-V$s are more asymmetric than for HG and explain this complicated behavior and broad $I-V$ distribution by the complexity of the end groups of TSC, enabling several contact geometries (see Supporting Information).

In order to deduce a microscopic understanding of the charge transport through these molecules, we apply the single-level (or resonant-level) transport model. The single-level model is based on the Landauer formula[2,44] assuming a single MO at energy E_0 from the Fermi energy E_F of the metal, coupled via the coupling constants Γ_L and Γ_R to the left and the right leads. The coupling results in a broadening of the level and yields a resonance with Lorentzian shape for the transmission function:[2,11,33−35]

$$T(E) = \frac{4\Gamma_L\Gamma_R}{[E - E_0]^2 + [\Gamma_L + \Gamma_R]^2} \quad (1)$$

The transmission at E_F corresponds to the conductance G in units of G_0, i.e., $G = G_0T(E_F)$. In general, the conducting MO is formed by either the HOMO or the LUMO of the molecule coupled to the electrodes, $E_0 = E_{HOMO/LUMO} - E_F$ with $E_{HOMO/LUMO}$ being the energy level of the HOMO or the LUMO. Each $I-V$ curve was fitted with this model, and the level alignment E_0 and the level broadening Γ were inferred from these fits. Since the majority of the $I-V$s turned out to be symmetric $\Gamma_R = \Gamma_L$, we use $\Gamma = \Gamma_R + \Gamma_L$ for the further discussion.[2,11,33−35]

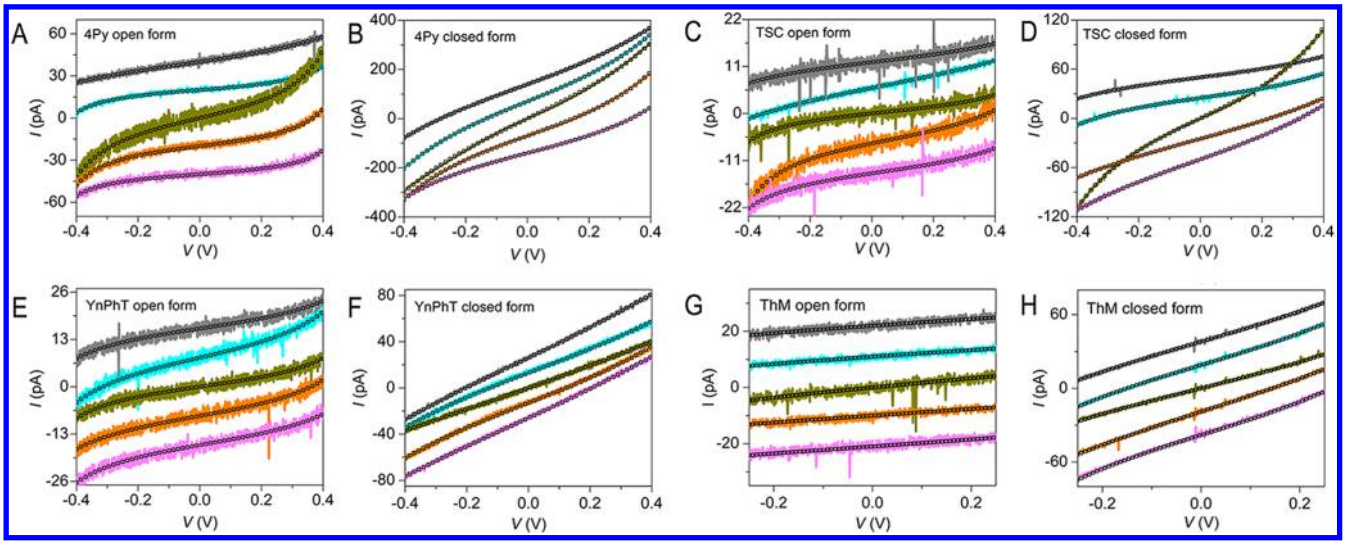

Figure 4. Representative $I-V$s (color) with corresponding fitting curves (black square) are presented for open (left panels) and closed (right panels) forms of four different species, 4Py (A, B), TSC (C, D), YnPhT (E, F), and ThM (G, H). For enhancing clarity, some of the curve pairs (experiment and fit) are vertically offset. The fitting parameters are (from top to bottom) (A) E_0 = 0.45 eV, Γ = 0.29 meV; E_0 = 0.26 eV, Γ = 0.12 meV; E_0 = 0.28 eV, Γ = 0.23 meV; E_0 = 0.26 eV, Γ = 0.16 meV; E_0 = 0.26 eV, Γ = 0.12 meV, (B) E_0 = 0.48 eV, Γ = 1.20 meV; E_0 = 0.40 eV, Γ = 1.03 meV; E_0 = 0.45 eV, Γ = 1.26 meV; E_0 = 0.36 eV, Γ = 0.88 meV; E_0 = 0.37 eV, Γ = 0.78 meV, (C) E_0 = 0.40 eV, Γ = 0.13 meV; E_0 = 0.55 eV, Γ = 0.24 meV; E_0 = 0.37 eV, Γ = 0.13 meV; E_0 = 0.31 eV, Γ = 0.14 meV; E_0 = 0.33 eV, Γ = 0.13 meV, (D) E_0 = 0.40 eV, Γ = 0.32 meV; E_0 = 0.36 eV, Γ = 0.29 meV; E_0 = 0.34 eV, Γ = 0.52 meV; E_0 = 0.54 eV, Γ = 0.62 meV; E_0 = 0.51 eV, Γ = 0.67 meV, (E) E_0 = 0.34 eV, Γ = 0.14 meV; E_0 = 0.34 eV, Γ = 0.17 meV; E_0 = 0.32 eV, Γ = 0.12 meV; E_0 = 0.35 eV, Γ = 0.15 meV; E_0 = 0.36 eV, Γ = 0.15 meV, (F) E_0 = 0.86 eV, Γ = 1.11 meV; E_0 = 0.59 eV, Γ = 0.69 meV; E_0 = 1.32 eV, Γ = 1.48 meV; E_0 = 0.54 eV, Γ = 0.63 meV; E_0 = 0.91 eV, Γ = 1.15 meV, (G) E_0 = 0.80 eV, Γ = 0.32 meV; E_0 = 0.95 eV, Γ = 0.39 meV; E_0 = 0.82 eV, Γ = 0.54 meV; E_0 = 0.83 eV, Γ = 0.33 meV; E_0 = 1.04 eV, Γ = 0.42 meV, (H) E_0 = 0.45 eV, Γ = 0.55 meV; E_0 = 0.39 eV, Γ = 0.49 meV; E_0 = 0.44 eV, Γ = 0.50 meV; E_0 = 0.47 eV, Γ = 0.60 meV; E_0 = 0.36 eV, Γ = 0.45 meV.

dx.doi.org/10.1021/nl3015523 | Nano Lett. XXXX, XXX, XXX−XXX

Table 2. Molecular Level Alignment (E_0) and Level Broadening ($\Gamma = \Gamma_L + \Gamma_R$) as Extracted from a Set of $I-V$ Curves by Use of the Single-Level Model[a]

	open form		closed form (eV)		difference (eV)	
	Γ (10^{-4} eV)	$\lvert E_0\rvert$ (10^{-1} eV)	Γ (10^{-4} eV)	$\lvert E_0\rvert$ (10^{-1} eV)	$\Delta\Gamma$ (10^{-4} eV)	$\Delta\lvert E_0\rvert$ (10^{-1} eV)
4Py	2.4 ± 1.2	3.5 ± 0.8	13.1 ± 3.2	4.2 ± 0.7	10.7 ± 3.4	0.7 ± 0.9
TSC	1.7 ± 0.7	4.1 ± 0.5	5.5 ± 1.8	6.0 ± 0.8	3.8 ± 1.9	1.9 ± 0.9
YnPhT	1.6 ± 0.3	3.7 ± 0.6	12.1 ± 3.4	10.0 ± 1.7	10.5 ± 3.4	6.3 ± 1.8
ThM	4.0 ± 1.0	8.6 ± 1.4	6.3 ± 1.2	5.4 ± 1.1	2.3 ± 1.6	−3.2 ± 1.8

[a]The values are plotted in Figure 5a,b. The given errors are the standard deviations. Differences $\Delta\Gamma = \Gamma_{closed} - \Gamma_{open}$ and $\Delta\lvert E_0\rvert = \lvert E_0\rvert_{closed} - \lvert E_0\rvert_{open}$ are given to elucidate the correlation with the conductance switching ratio in Table 1.

In Figure 4, examples of $I-V$s and the corresponding fitting curves are presented for open and closed forms of all species, 4Py, TSC, YnPhT, and ThM. We find that the single-level model reproduces the $I-V$ curves very reliably throughout the whole voltage range with slight variation in the fit parameters, though. The averaged values for E_0 and Γ are listed in Table 2. A more detailed discussion for the complex closed state of TSC is given in the Supporting Information.

Within the voltage range accessible by our measurement, eq 1 can be well described by the sum of a linear and a cubic term of the voltage with both prefactors being dependent on Γ and E_0 as it is nicely discussed in a recent publication.[35] Because of the weak nonlinearity of the $I-V$s, the independent determination of Γ and E_0 by fitting is not obvious. We therefore performed various numerical tests to ensure the stability of our fits (see Supporting Information). In addition, it should be noted that the fits provide no information about the sign of E_0 and can thus not reveal whether the frontier MO is the LUMO or the HOMO.

As shown in Figure 5A, the level broadening Γ is bigger in the closed isomers than in the open ones for all four species. In the experiments, Γ of ThM, with the nonconjugated side chain, shows only a small difference between open and closed forms, while the Γ values of the conjugated molecules exhibit significant differences of more than a factor of 3 (see Table 2). This indicates that the delocalization of the frontier MO in the closed form enhances the coupling strength. Moreover, the values of SR follow the order of the difference $\Delta\Gamma = \Gamma_{closed} - \Gamma_{open}$, indicating that $\Delta\Gamma$ essentially determines SR.

The molecular level alignment E_0 in Figure 5B shows a more complex behavior. Naively, one expects that the frontier MO in the open form is separated further from E_F than in the closed form because the breaking of the conjugation due to the opening of the ring enlarges the HOMO−LUMO gap, as confirmed by our electronic structure calculations for the isolated molecules in the Supporting Information. The situation is sketched in Figure 5C.[43,45,46] This scenario is in fact observed for the ThM molecule containing a nonconjugated side chain. Surprisingly, the measurements in Figure 5B show that the frontier MOs of the closed form for the conjugated molecules 4Py, TSC, and YnPhT exhibit larger values of E_0 (i.e., the levels are further away from E_F) than in the respective open forms. The related changes in level alignment and broadening are illustrated in Figure 5D. Since this more off-resonant transport situation goes along with a strongly increased Γ, a higher transmission of the closed form is still the result. As can be deduced from Tables 1 and 2, there is no correlation between E_0 and SR.

The observed changes of both E_0 and Γ between open and closed forms differ markedly from molecule to molecule. From this finding we conclude that the molecular coupling to the

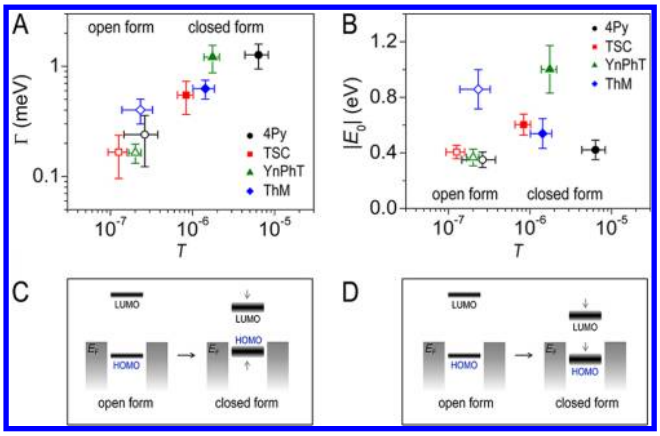

Figure 5. Fitting parameters of the single-level model (A) Γ and (B) E_0 obtained as an average over the parameters extracted from 20 individual $I-V$ curves for each molecule and displayed as a function of the transmission determined by eq 1. Vertical error bars indicate the respective standard deviation. Horizontal error bars are the standard deviation of the transmission as deduced from the variations of Γ and E_0. Open and closed symbols indicate the open and closed form of the molecules, respectively. (C) Illustration of the changes of the MOs from the open to the closed form for the "nonconjugated" molecule ThM. In the closed form, HOMO and LUMO levels move upward and downward, respectively. The HOMO−LUMO gap narrows and molecular levels broaden. (D) Same as panel C but for the "conjugated" molecules 4Py, TSC, and YnPhT. In the closed form, both HOMO and LUMO levels move downward, while the HOMO−LUMO gap simultaneously narrows and the molecular levels broaden.

electrodes and the exact positions of HOMO and LUMO levels depend strongly on the side chains and end groups of these diarylethene molecules. Moreover, the conductance switching of diarylethene molecules is dominated by the changes of Γ rather than those of E_0 because a more extended π-system significantly enhances the strength of the coupling irrespective of the level alignment.

In conclusion, we have investigated charge transport characteristics of photochromic molecules using the MCBJ technique at low temperatures. We have developed four different types of diarylethene molecules with a sulfur-free switching core to reduce the possibility of unintended binding. UV/vis spectroscopy and density functional theory calculations were performed, which show that the nonconjugated ThM molecule behaves differently compared to the conjugated molecules 4Py, TSC, and YnPhT. The single-molecule conductance has been examined while breaking and forming the atomic contacts repeatedly. This reveals that both the conduction properties and the conductance switching ratios are significantly influenced by the end groups and by the side chains of the molecules. By analyzing the $I-V$ curves within the

dx.doi.org/10.1021/nl3015523 | Nano Lett. XXXX, XXX, XXX−XXX

framework of the single-level transport model, we find that the alignment of the dominant transport level and the level broadening vary unambiguously between open and closed forms and that the delocalization of the π-electron system significantly amplifies the coupling. The higher conductance values of the closed forms of the diarylethene molecules as compared to the open ones are explained by the strong increase in this broadening, which overcompensates even a more off-resonant transport situation found in some cases for the closed forms. These findings are crucial for the development of functional nanoscale electronics for applications in physics, chemistry, and material engineering and future molecular electronic devices.

■ ASSOCIATED CONTENT

Supporting Information

Details on experimental procedures and theoretical methods. This material is available free of charge via the Internet at http://pubs.acs.org.

■ AUTHOR INFORMATION

Corresponding Author

*E-mail: elke.scheer@uni-konstanz.de.

Present Address

[⊥]Molecular Foundry, Lawrence Berkeley National Laboratory, Berkeley, CA 94720.

Notes

The authors declare no competing financial interest.

■ ACKNOWLEDGMENTS

We thank J. C. Cuevas, P. Leiderer, B. Briechle, T. Exner, and J. Boneberg for fruitful discussions. The work in Konstanz was supported by the Deutsche Forschungsgemeinschaft through SFB767 and the Ministry of Research and the Arts of Baden-Württemberg within the Center for Applied Photonics. The authors are also grateful to MCAT for a generous gift of Bestmann-Ohira reagent. T.J.H. and F.P. were funded through the Baden-Württemberg Stiftung within the Network of Excellence "Functional Nanostructures" and the Center for Functional Nanostructures, Project C3.6.

■ REFERENCES

(1) Nitzan, A.; Ratner, M. A. *Science* **2003**, *300* (5624), 1384−1389.

(2) Cuevas, J. C.; Scheer, E. *Molecular Electronics: An Introduction to Theory and Experiment*. World Scientific: Singapore, 2010.

(3) Del Valle, M.; Gutiérrez, R.; Tejedor, C.; Cuniberti, G. *Nat. Nanotechnol.* **2007**, *2* (3), 176−179.

(4) Song, H.; Kim, Y.; Jang, Y. H.; Jeong, H.; Reed, M. A.; Lee, T. *Nature* **2009**, *462* (7276), 1039−1043.

(5) Venkataraman, L.; Klare, J. E.; Nuckolls, C.; Hybertsen, M. S.; Steigerwald, M. L. *Nature* **2006**, *442* (7105), 904−907.

(6) Xu, B. Q.; Xiao, X. Y.; Yang, X. M.; Zang, L.; Tao, N. J. *J. Am. Chem. Soc.* **2005**, *127* (8), 2386−2387.

(7) Chen, F.; He, J.; Nuckolls, C.; Roberts, T.; Klare, J. E.; Lindsay, S. *Nano Lett.* **2005**, *5* (3), 503−506.

(8) Pobelov, I. V.; Li, Z. H.; Wandlowski, T. *J. Am. Chem. Soc.* **2008**, *130* (47), 16045−16054.

(9) Champagne, A. R.; Pasupathy, A. N.; Ralph, D. C. *Nano Lett.* **2005**, *5* (2), 305−308.

(10) Kim, Y.; Song, H.; Strigl, F.; Pernau, H. F.; Lee, T.; Scheer, E. *Phys. Rev. Lett.* **2011**, *106* (19), 196804.

(11) Kim, Y.; Pietsch, T.; Erbe, A.; Belzig, W.; Scheer, E. *Nano Lett.* **2011**, *11* (9), 3734−3738.

(12) Li, C.; Pobelov, I.; Wandlowski, T.; Bagrets, A.; Arnold, A.; Evers, F. *J. Am. Chem. Soc.* **2008**, *130* (1), 318−326.

(13) Zhu, L.; Yao, K. L.; Liu, Z. L. *Appl. Phys. Lett.* **2010**, *97* (20), 202101.

(14) Matsuda, K.; Irie, M. *J. Am. Chem. Soc.* **2000**, *122* (30), 7195−7201.

(15) Jo, M. H.; Grose, J. E.; Baheti, K.; Deshmukh, M. M.; Sokol, J. J.; Rumberger, E. M.; Hendrickson, D. N.; Long, J. R.; Park, H.; Ralph, D. C. *Nano Lett.* **2006**, *6* (9), 2014−2020.

(16) Bogani, L.; Wernsdorfer, W. *Nat. Mater.* **2008**, *7* (3), 179−186.

(17) van der Molen, S. J.; Liao, J. H.; Kudernac, T.; Agustsson, J. S.; Bernard, L.; Calame, M.; van Wees, B. J.; Feringa, B. L.; Schönenberger, C. *Nano Lett.* **2009**, *9* (1), 76−80.

(18) Dulić, D.; van der Molen, S. J.; Kudernac, T.; Jonkman, H. T.; de Jong, J. J. D.; Bowden, T. N.; van Esch, J.; Feringa, B. L.; van Wees, B. J. *Phys. Rev. Lett.* **2003**, *91* (20), 207402.

(19) Whalley, A. C.; Steigerwald, M. L.; Guo, X.; Nuckolls, C. *J. Am. Chem. Soc.* **2007**, *129* (42), 12590−12591.

(20) de Jong, J. J. D.; Lucas, L. N.; Kellogg, R. M.; van Esch, J. H.; Feringa, B. L. *Science* **2004**, *304* (5668), 278−281.

(21) Irie, M.; Kobatake, S.; Horichi, M. *Science* **2001**, *291* (5509), 1769−1772.

(22) Kronemeijer, A. J.; Akkerman, H. B.; Kudernac, T.; van Wees, B. J.; Feringa, B. L.; Blom, P. W. M.; de Boer, B. *Adv. Mater.* **2008**, *20* (8), 1467−1473.

(23) Uchida, K.; Yamanoi, Y.; Yonezawa, T.; Nishihara, H. *J. Am. Chem. Soc.* **2011**, *133* (24), 9239−9241.

(24) Katsonis, N.; Kudernac, T.; Walko, M.; van der Molen, S. J.; van Wees, B. J.; Feringa, B. L. *Adv. Mater.* **2006**, *18* (11), 1397−1400.

(25) He, J.; Chen, F.; Liddell, P. A.; Andréasson, J.; Straight, S. D.; Gust, D.; Moore, T. A.; Moore, A. L.; Li, J.; Sankey, O. F.; Lindsay, S. M. *Nanotechnology* **2005**, *16* (6), 695−702.

(26) Tam, E. S.; Parks, J. J.; Shum, W. W.; Zhong, Y. W.; Santiago-Berrios, M. B.; Zheng, X.; Yang, W. T.; Chan, G. K. L.; Abruna, H. D.; Ralph, D. C. *ACS Nano* **2011**, *5* (6), 5115−5123.

(27) Park, Y. S.; Widawsky, J. R.; Kamenetska, M.; Steigerwald, M. L.; Hybertsen, M. S.; Nuckolls, C.; Venkataraman, L. *J. Am. Chem. Soc.* **2009**, *131* (31), 10820−10821.

(28) Sako, E. O.; Kondoh, H.; Nakai, I.; Nambu, A.; Nakamura, T.; Ohta, T. *Chem. Phys. Lett.* **2005**, *413* (4−6), 267−271.

(29) Boscoboinik, J. A.; Kohlmeyer, R. R.; Chen, J.; Tysoe, W. T. *Langmuir* **2011**, *27* (15), 9337−9344.

(30) Sysoiev, D.; Fedoseev, A.; Kim, Y.; Exner, T. E.; Boneberg, J.; Huhn, T.; Scheer, E.; Leiderer, P.; Scheer, E.; Groth, U.; Steiner, U. E. *Chem.—Eur. J.* **2011**, *17* (24), 6663−6672.

(31) Zhuang, M.; Ernzerhof, M. *J. Chem. Phys.* **2009**, *130* (11), 114704.

(32) Jakobsson, F. L. E.; Marsal, P.; Braun, S.; Fahlman, M.; Berggren, M.; Cornil, J.; Crispin, X. *J. Phys. Chem. C* **2009**, *113* (42), 18396−18405.

(33) Zotti, L. A.; Kirchner, T.; Cuevas, J. C.; Pauly, F.; Huhn, T.; Scheer, E.; Erbe, A. *Small* **2010**, *6* (14), 1529−1535.

(34) Huisman, E. H.; Guédon, C. M.; van Wees, B. J.; van der Molen, S. J. *Nano Lett.* **2009**, *9* (11), 3909−3913.

(35) Hong, W. J.; Valkenier, H.; Meszaros, G.; Manrique, D. Z.; Mishchenko, A.; Putz, A.; Garcia, P. M.; Lambert, C. J.; Hummelen, J. C.; Wandlowski, T. *Beilstein J. Nanotechnol.* **2011**, *2*, 699−713.

(36) Browne, W. R.; de Jong, J. J. D.; Kudernac, T.; Walko, M.; Lucas, L. N.; Uchida, K.; van Esch, J. H.; Feringa, B. L. *Chem.—Eur. J.* **2005**, *11* (21), 6414−6429.

(37) Kushmerick, J. G.; Lazorcik, J.; Patterson, C. H.; Shashidhar, R.; Seferos, D. S.; Bazan, G. C. *Nano Lett.* **2004**, *4* (4), 639−642.

(38) Chen, F.; Li, X. L.; Hihath, J.; Huang, Z. F.; Tao, N. J. *J. Am. Chem. Soc.* **2006**, *128* (49), 15874−15881.

(39) Li, X. L.; He, J.; Hihath, J.; Xu, B. Q.; Lindsay, S. M.; Tao, N. J. *J. Am. Chem. Soc.* **2006**, *128* (6), 2135−2141.

(40) Li, Z. H.; Pobelov, I.; Han, B.; Wandlowski, T.; Blaszczyk, A.; Mayor, M. *Nanotechnology* **2007**, *18* (4), 044018.

(41) Quek, S. Y.; Kamenetska, M.; Steigerwald, M. L.; Choi, H. J.; Louie, S. G.; Hybertsen, M. S.; Neaton, J. B.; Venkataraman, L. *Nat. Nanotechnol.* **2009**, *4* (4), 230−234.
(42) Zhou, X. S.; Chen, Z. B.; Liu, S. H.; Jin, S.; Liu, L.; Zhang, H. M.; Xie, Z. X.; Jiang, Y. B.; Mao, B. W. *J. Phys. Chem. C* **2008**, *112* (10), 3935−3940.
(43) Li, J.; Speyer, G.; Sankey, O. F. *Phys. Rev. Lett.* **2004**, *93* (24), 248302.
(44) Büttiker, M.; Imry, Y.; Landauer, R.; Pinhas, S. *Phys. Rev. B* **1985**, *31* (10), 6207−6215.
(45) Tsuji, Y.; Staykov, A.; Yoshizawa, K. *J. Phys. Chem. C* **2009**, *113* (52), 21477−21483.
(46) Huang, J.; Li, Q.; Ren, H.; Su, H.; Shi, Q. W.; Yang, J. *J. Chem. Phys.* **2007**, *127* (9), 094705.

dx.doi.org/10.1021/nl3015523 | *Nano Lett.* XXXX, XXX, XXX−XXX